Available online at www.sciencedirect.com
SCIENCE DIRECT®
Talanta 67 (2005) 286–303
Talanta
www.elsevier.com/locate/talanta

Applications of synchrotron radiation in forensic trace evidence analysis

Ivan M. Kempson [a,*], K. Paul Kirkbride [b], William M. Skinner [a], John Coumbaros [b]

[a] *Ian Wark Research Institute, University of South Australia, Mawson Lakes, SA 5095, Australia*
[b] *Forensic Science, SA, 21 Divett Place, Adelaide, SA 5000, Australia*

Available online 11 July 2005

Abstract

Synchrotron radiation sources have proven to be highly beneficial in many fields of research for the characterization of materials. However, only a very limited proportion of studies have been conducted by the forensic science community. This is an area in which the analytical benefits provided by synchrotron sources could prove to be very important. This review summarises the applications found for synchrotron radiation in a forensic trace evidence context as well as other areas of research that strive for similar analytical scrutiny and/or are applied to similar sample materials. The benefits of synchrotron radiation are discussed in relation to common infrared, X-ray fluorescence, tomographic and briefly, X-ray diffraction and scattering techniques. In addition, X-ray absorption fine structure analysis (incorporating XANES and EXAFS) is highlighted as an area in which significant contributions into the characterization of materials can be obtained. The implications of increased spatial resolution on microheterogeneity are also considered and discussed.

Keywords: Synchrotron radiation; Infrared; XAFS; XANES; EXAFS; Microheterogeneity; X-ray tomography; Trace evidence; Impurity profiling; GSR

1. Introduction

This review describes the production of synchrotron radiation, summarises the impact that synchrotron light sources have made upon forensic science, and indicates potential applications through citation of relevant examples from the wider analytical chemistry field. The articles featured suggest that forensic science could benefit from the unique capabilities synchrotron facilities promise for analysis of trace material with greater spatial resolution, more rapid analysis and higher sensitivity.

Synchrotron radiation offers a superior light source for many conventional 'photon in' techniques that could play a major role in trace evidence analysis. This would allow greater sensitivity and analysis of much lower concentrations and smaller samples than typically possible. As such, synchrotron sources are relevant to forensic science trace evidence analysis when: conventional techniques fail due to limits of detection; added scrutiny and discrimination is required such as in high profile cases; to perform fundamental research into 'evidence material science'. Demonstrations of superior sensitivity and resolving power are presented here that portray the benefits of synchrotron sources in fields such as materials research. In addition, areas of current forensic research are identified where application of synchrotron radiation could greatly assist interpretation, for example the composition and structure of gunshot residues and identifying other discriminatory vibrational bands in paints and fibres.

Increasing analytical sensitivity gives rise to an ability to study smaller samples or volumes/areas within a specimen. Following from this however, is the emergence of additional instrumental and analytical complexities. Although the instrumental implications are beyond the focus of this review, some of the considerations for deriving analytical conclusions will be discussed. For example, one area of primary concern is the limit of heterogeneity in a sample and the point at which microscopic samples cease to be representative of the original source, i.e. the impact of microheterogeneity.

* Corresponding author. Tel.: +61 8 8302 3495; fax: +61 8 8302 3683.
E-mail address: ivan.kempson@unisa.edu.au (I.M. Kempson).

0039-9140/$ – see front matter © 2005 Elsevier B.V. All rights reserved.
doi:10.1016/j.talanta.2005.05.026

This is an area of active research which has particular relevance to forensic analysis and for which synchrotrons are ideally suited.

2. Synchrotron radiation

Synchrotron radiation is emitted by charged particles travelling in curved trajectories at relativistic speeds (near the speed of light). This process is exploited in a synchrotron facility, a purpose-built machine that hosts an energetic beam of electrons or positrons in a closed loop (the remainder of this section will refer only to electron beams). The heart of a synchrotron is the storage ring that confines the beam in vacuum around a polygonal course with magnets bending the beam around each apex of the ring (see Fig. 1). Radiation is emitted in a direction tangential to the electron trajectory with a high degree of collimation. The ring is "injected" with electrons either periodically or continuously from a booster ring at the appropriate energy, which is in turn fed by a linear accelerator. The electromagnetic radiation that is emitted at each bend covers a broad range of the spectrum from the infrared region through visible, ultraviolet, X-rays to gamma rays. The radiation is accessed via beamlines that include optics for focusing and monochromation (wavelength selection), and the experimental end-station. The rest of the storage ring comprises devices for maintaining beam confinement and for replenishing the energy lost by the beam upon radiation.

The intensity and wavelength range of the emitted radiation may be modified by the inclusion of "insertion devices" in the straight sections of the storage ring. Each straight section can have one or more insertion devices, which have no net affect on the direction of the electron beam but involve a series bends that give rise to an accumulative radiative process. These involve a series of magnetic fields that induce periodic accelerations in the electron beam, thus enhancing the emitted light intensity. The simplest of these devices is termed a "Wiggler" which produces a semi-continuous spectrum. If the period of the alternating magnet poles and their strength are chosen correctly, constructive interference may be exploited and a pseudo-monochromatic radiation beam of even higher brightness and laser-like properties may be produced. Insertion devices of this type are termed "undulators".

The combination of storage ring energy, insertion devices and beamline optics allows the characteristics and properties of synchrotron radiation to be varied and controlled. These properties include:

- *Brightness (i.e. flux per unit area)*. The brightness of the photon beam can be several orders of magnitude greater than any conventional laboratory source (Fig. 2). This unparalleled intensity enables extremely rapid measurements to be made. Furthermore, with use of appropriate beamline optics, samples and features as small as a few tens of nanometers may be probed efficiently in experiments utilising short-wavelength radiation such as X-ray fluorescence, photoemission and absorption spectroscopic techniques, imaging and X-ray diffraction.
- *Tunability*. Discrete wavelengths at extremely high resolving power ($E/\Delta E$) can be selected using appropriate monochromators (gratings, crystals) on the experimental beamline. This is extremely powerful as it allows a whole unique class of measurements to be performed; namely X-

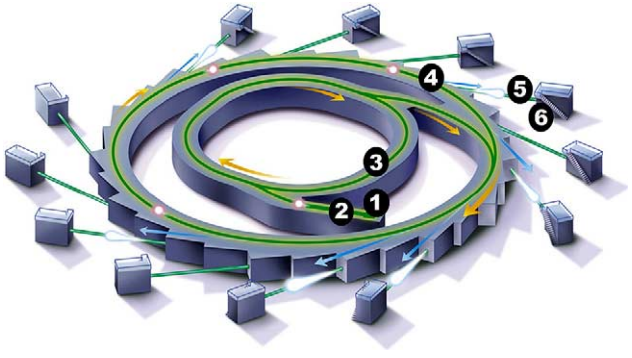

Fig. 1. Layout of the Australian Synchrotron showing: (1) electron source, (2) linear accelerator (LINAC), (3) booster ring, (4) storage ring, (5) beamline and (6) experimental endstation. Figure courtesy Australian Synchrotron Project.

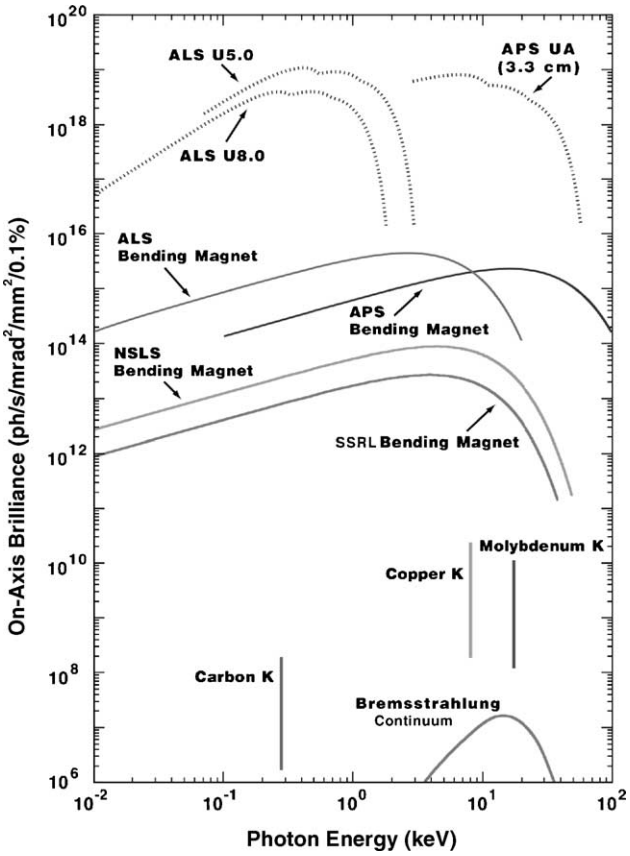

Fig. 2. Comparative on-axis brilliance and spectral range of synchrotron insertion device and bending magnet sources compared to conventional sources. Provided courtesy of R. Fenner, Argonne National Laboratories.

ray absorption spectroscopy (XAS) in which the exciting photon energy is scanned across an element absorption edge (see Section 4). 2D and 3D (tomographic) X-ray imaging techniques can also exploit tunability to enhance contrast by comparing data collected at wavelengths above and below an adsorption edge. Spectroscopic interferences may also be minimized in this way.

- *Polarization*. Synchrotron radiation is normally linearly polarized in the orbital plane and elliptically polarized above and below the orbital plane. Certain insertion devices may also be used to alter the polarization as desired. This characteristic of synchrotron light can be exploited to provide orientation information by altering either the polarization (via the insertion device) or the beam-sample geometry.
- *Time-resolved*. The energy of the electron beam, which is lost during synchrotron radiation emission, is replenished by an oscillating voltage in radio frequency (rf) cavities situated within the storage ring. The result is a periodic "bunching" of electrons with a variable frequency depending on the cavity frequency and circumference of the storage ring. Time-resolved measurements are then possible using the resultant pulses of synchrotron radiation, which may be shorter than a ns with μs^{-1} to ns^{-1} repletion rates [1].
- *Coherence*. Laser-like properties result from the constructive interference produced by undulators (as described above) [1].
- *Non-destructive*. This is possibly the most important aspect for forensic investigations. For the majority of trace forensic evidence (e.g. contact traces such as paint flakes, glass fragments, hair and fibres, metal fragments, soils, stains), little, if any, sample preparation is required. The evidence may thus be analysed by other techniques or the analysis repeated if the results are contested.

The combination of unique and controllable source properties enables a broad range of experimental techniques. Conventional laboratory techniques such as X-ray diffraction (XRD) and X-ray fluorescence (XRF), infrared (IR), photoemission and ultraviolet (UV) spectroscopies, may be performed much more rapidly with enhanced signal-to-noise ratios. Coupled with high performance monochromation, the high brightness results in great improvements in spectral resolution. Efficient focusing also allows bright photon beams to be concentrated on spot sizes down to tens of nm in X-ray applications and diffraction limited spots for IR spectroscopy. In the context of forensic science, reliable and information-rich data may be obtained from extremely small samples of material. Most importantly, new measurements are made possible by the use of synchrotron radiation. One such technique is X-ray absorption spectroscopy (XAS), which utilises the tunability of synchrotron sources. XAS and its applicability to forensic analysis will be discussed in Section 4.

Over 50 synchrotron radiation facilities exist worldwide. Of these, first generation rings were initially utilised in the 1960s. These rings were originally designed as accelerators for high-energy particle physics, but when it was realised that the detrimental loss of energy as electromagnetic radiation was a novel, bright source for analytical probes, 'parasitic' beamlines emerged. Second generation facilities emerged in the late 1970s and early 1980s, which were built as dedicated synchrotron radiation sources. Third generation sources have been appearing since the early to mid 1990s. SPring-8 (Japan), the Advanced Photon Source (APS, USA, Fig. 3) and the European Synchrotron Radiation Facility (ESRF, Grenoble, France) are currently the premier examples of third generation sources that have been designed to optimise the use of insertion devices to produce the brightest beams currently available. Each of these operates at energies of 8, 7 and 6 GeV, respectively.

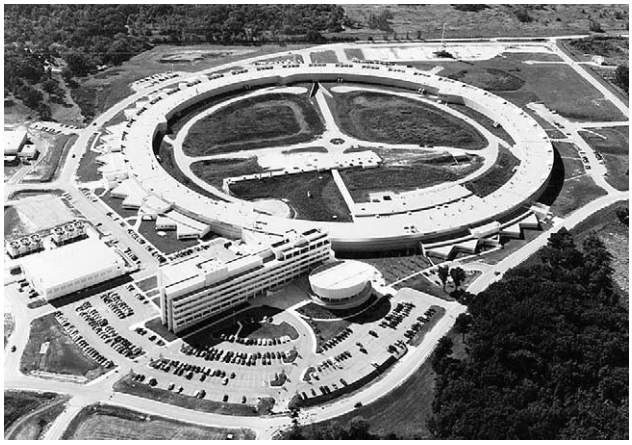

Fig. 3. An aerial view of the Advanced Photon Source synchrotron at Argonne National Laboratories, IL, USA. Provided courtesy of R. Fenner, Argonne National Laboratories.

Numerous techniques that utilise incident electromagnetic radiation are available at synchrotron sources. A selection of references has been included throughout this review, where relevant, that deals explicitly with specific beam lines and are useful for reference to individual line capabilities, applications and instrumentation. These references give an overview of typical beamlines available at many synchrotrons but are by no means exhaustive.

Access to a synchrotron facility has been somewhat limited and would not necessarily be available for routine analysis. This is due to the limited numbers of synchrotron facilities, and as a consequence, user demand for the available facilities is high and there are high costs associated for external agencies that 'purchase' access. However, as many of the major synchrotron techniques have matured and hardware for unattended analysis developed, rapid access mechanisms have been increasingly implemented, e.g. the synchrotron radiation source (SRS, Daresbury, UK). Indeed, newer facilities under construction at present, have actively sought industry and public agency advice in the setting up of access management structures. The Canadian Light Source (CLS) and the Australian Synchrotron Project are examples.

3. Synchrotron infrared (IR)

In keeping with the general characteristics of synchrotron radiation, IR beams exhibit extreme brightness. Additionally, the output profile of the source is quite "flat", decaying to only one-half of peak output over the 1–1000 μm range. A Globar source, by comparison, decays by four orders of magnitude over the same range. As a consequence, if a spectrometer equipped with a synchrotron source has an appropriate range of beamsplitters and detectors, near IR, mid IR and far IR experiments can be conducted. However, as the beam has extremely low divergence and very small diameter, the interaction between the beam and the specimen occurs over a very small domain. As a consequence, spectrometers equipped with a synchrotron source do not offer increased performance compared to conventional spectrometers for analysis of large specimens, except in the far IR range where the extreme brightness of the source does afford a performance advantage despite the small beam diameter. Compared to conventional systems, however, a synchrotron source equipped with a microspectrometer does offer unrivalled performance in the mid IR region for very small specimens or small features within specimens (e.g. smaller than about 50 μm). As infrared microspectroscopy in this spectral region is of great relevance to the trace evidence examiner, this section will be limited to that subject.

High performance for IR microspectroscopy arises though superior signal-to-noise ratio capability and better diffraction characteristics. In relation to the former, Carr et al. [2] has found that the noise applicable to synchrotron sources is about 20 times smaller than noise from a Globar source. Reffner and Martoglio [3] indicates that the low noise inherent to synchrotron IR radiation is due to the fact that it originates from a source that is not thermal and is not therefore subject to Boltzmann noise. Therefore, an acquisition requiring 4 min with a microspectrometer equipped with a synchrotron source would take about 400 times longer (at least a day) on a conventional microspectrometer in order to attain equivalent noise. While the inherent noise of a synchrotron source is very low, the signal received by the detector can be extremely high due to the brightness of the source. As a consequence signal-to-noise ratios can be extremely high. Carr et al. [2] indicates that the level of brightness can be three orders of magnitude greater than that for a Globar. Dumas and Williams [4] has calculated that as a result of source brightness, the use of a synchrotron as an IR source offers an advantage of 1-million to one over a Globar source as far as signal-to-noise is concerned. From Dumas' calculations, a 1 s measurement with a synchrotron source is equivalent to an 11 day measurement with a conventional source.

In relation to diffraction, with conventional IR microscopes, a relatively dull beam tens of millimeters in diameter is brought into focus in a spot approximately 100–200 μm in diameter at the specimen plane. In order to analyse specimens smaller than the beam diameter, or avoid collection of unwanted spectral data from certain regions of a heterogenous specimen, diaphragms ("apertures") must be established at one or more of the focal planes in the microscope to trim the beam dimensions. In trace evidence examination, where thin fibres, tiny mineral inclusions within a paint binder matrix, or paint cross-sections comprising thin films are encountered, it is necessary to delineate specimens a few or few tens of microns across. Under these circumstances the radiation throughput is extremely low. Moreover, the narrow slit through which the beam passes is of approximately the same size as the wavelength of the probing radiation (10 μm corresponds to 1000 cm^{-1}, which is within the mid-IR region), therefore the beam suffers considerable diffraction. This causes a significant proportion of the beam to impact outside the region delineated by the diaphragms. In the case that a homogeneous but microscopic specimen is under examination, such as a thin fibre, the diffracted radiation passes though the air surrounding the specimen and is therefore recorded as stray radiation with some negative impact upon the photometric accuracy of the spectral data. However, when heterogeneous specimens such as paint cross-sections are examined, the diffracted radiation will impact outside the desired analytical area with the result of "spectral leakage" from the adjacent areas, contaminating the spectral data of the target region. Synchrotron beams are extremely narrow and suffer from extremely low divergence (approximately 80 mrad horizontally by 40 mrad vertically [5]); in essence the effective source size is about 100 μm compared to many millimeters for a conventional source [6]. Once it is passed through the optics of an IR microscope, the beam produces an illuminated area of about 15 μm × 20 μm at the stage of the microscope. This is about two orders of magnitude smaller that the illuminated area in the same microscope equipped with a Globar source [2]. With a synchrotron source, the impact of diffraction is much less than with a Globar source, allowing microspectrometers equipped with a synchrotron source to record good spectral data through diaphragms set to 10 μm^2 or even less. For comparison, the limit of performance for microscopes equipped with conventional sources is approximately 30 μm [6]. Reffner and Williams has estimated that equipping IR microspectrometers with a synchrotron source increases performance at the diffraction limit by about 40–100 times [3]. Obviously if a specimen or a feature of about 100 μm is placed at the focus of an IR microspectrometer equipped with a synchrotron source then a substantial fraction of the specimen will not be interrogated by the beam. For specimens of this size conventional microspectrometers offer approximately equivalent performance because the beam is so much larger, even though it is less bright.

Further performance developments in IR microspectrometers equipped with synchrotron sources are likely. Carr et al. [2] indicates that current IR microscopes are not optimized for synchrotron beam characteristics and that a change in the shape of reflecting optics from spherical to ellipsoidal would allow focussing of the beam to a spot size of about 2–10 μm at the stage. Conventional MCT detectors

have detector elements of approximately 250 μm × 250 μm size. As a consequence the narrow beam arising from a synchrotron "under-fills" such a detector. Greater signal-to-noise performance using synchrotrons can be achieved if the newer, smaller detector elements are utilized.

As well as transmission IR microspectroscopy in the mid-IR range, the extreme brightness of synchrotron sources should offer performance advantages in other experiments. For example, IR microspectroscopy in reflectance mode for microscopic specimens (i.e. approximately 50 μm or smaller) could prove a valuable technique. The high brightness of the source should allow infrared microspectroscopy to be conducted down to perhaps 100 cm^{-1}, assuming the microscope is equipped with a bolometer. Obviously, the impacts of diffraction are far worse in this region than in the mid IR, therefore the spatial resolution will be of the order of 100 μm or greater.

Although synchrotron hardware is extremely expensive and sophisticated, the IR microscopes, optical benches, detectors, and associated software are of the kind commonly found in forensic labs. Specimen preparation and handling requirements are therefore not unusual. In order to achieve the absolute best results from a microscope equipped with a synchrotron, some attention to detail regarding focusing and configuration of apertures is required; Carr has published an excellent article on this matter [7].

What follows is a discussion of specific examples of IR microspectroscopy using synchrotron sources in the literature, either forensic applications or those in allied fields that indicate a potential application in forensic trace evidence analysis. Several workers have demonstrated the capability offered by synchrotron IR microspectrometers for high signal-to-noise operation at or below the conventional diffraction limit; this utility is possibly the one of greatest relevance to the trace evidence analyst. Kalasinsky [8] used synchrotron IR microspectroscopy to detect and map the distribution of cocaine and 6-acetylmorphine in hair. Although the signals were subtle, cocaine at a concentration of 150 ng/mg (as ascertained by GC–MS) was detected by Kalasinsky. The mapping experiments conducted on longitudinally sectioned hairs indicated that cocaine was concentrated in the region of the medulla and depleted in the cortex, confirming earlier findings by the same author suggesting that hydrophobic drugs accumulate in the medulla while hydrophilic drugs tend to be distributed in the cortex. The ability to identify minute inclusions in a matrix has also been illustrated by Dumas [9], who also examined human hair. Microscopic nodules residing in the medulla were found to be rich in fatty acids. Dumas then used synchrotron X-ray fluorescence microscopy on the same specimens to indicate that the nodules were rich in calcium (also observed by Kempson et al. [10]), leading to the hypothesis that the nodules were calcium "soaps". Dumas also imaged the C=O band (1740 cm^{-1}) from individual, necrotic (dying) cells [9] and was able to identify the presence of oxidized proteins in the cytoplasm around the nucleus while the nucleus itself was virtually unaffected. Studies conducted

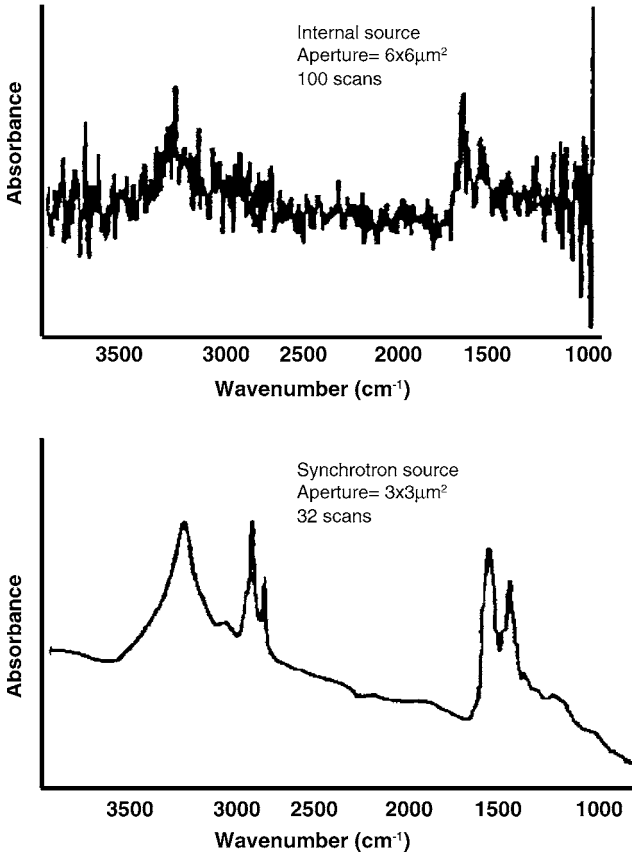

Fig. 4. Comparative IR absorbance spectra obtained from the same individual cell utilising a conventional and synchrotron sources. Reprinted, with permission, from [9], copyright by EDP Sciences, Les Ulis.

by Dumas employed 3 μm × 3 μm diaphragms to record the data, a feat that is not possible with conventional instruments. Therefore, whereas conventional IR microspectroscopy work dealing with necrotic tissue on a scale covering several cells indicated that oxidation was taking place somewhere in the specimen, synchrotron IR microspectroscopy allowed resolution of oxidation processes within a single cell. Fig. 4, after Dumas [9], demonstrates the ability to collect data of high signal-to-noise ratio using small diaphragms and a synchrotron source. The spectrum recorded on a conventional instrument required a sampling area four times bigger and three times the number of scans.

An article by Wilkinson et al. [11] indicates the potential for extremely energy-limited experiments of direct forensic interest: synchrotron specular reflectance IR microspectroscopy of inks on paper. The spatial resolution allows analysis of a single ink dot, and the high signal-to-noise ratio allows the identification of individual vibrational bands. Most significantly, the technique allows for non-destructive analysis of the ink specimen in situ, compared to other methods that call for extraction of ink components with the attendant risk that some chemical information might be discriminated against. Wilkinson et al., in another article [12], describes the use of synchrotron reflectance IR microspectroscopy to study,

characterize, and discriminate 25-year-old inks on Canadian stamps. By extension, it would appear that synchrotron reflectance IR microspectroscopy would have application for the analysis of not just inks on paper but other coatings such as photocopier toner and printer toners, especially those filled with carbon black that absorb IR very strongly. Synchrotrons allow the rapid collection of high resolution IR images at high signal-to-noise, this technique might have application in the mapping of inks or coatings on documents for the purpose of pictorially indicating where alterations have taken place.

Wilkinson et al. [13] conducted other experiments that highlighted the signal-to-noise advantage offered by synchrotron microspectroscopy for the analysis of microscopic features, he characterised components found in human fingerprints. In the same article Wilkinson describes analysis of fingerprints with X-ray fluorescence in order to map electrolytes. The goal of Wilkinson's work was to develop advanced methods for visualization of complex, partial prints, including those of pre-pubescent children.

Suzuki [14] has indicated that the extended mid-IR region (220–700 cm^{-1}) contains useful information for the forensic discrimination of paints. Minerals such as silicon dioxide, titanium dioxide and ferric oxide yield characteristic bands in this region allowing their positive identification and classification of crystalline form. Merill and Bartick [15] have also indicated that extended range IR is useful for the discrimination of pressure-sensitive adhesive tapes based upon inorganic material content (e.g. fillers, cross-linkers, and colour enhancers). With the exception of acrylate resins, the extended mid-IR region does not contain useful absorptions arising from paint binders. This carries through to the wider field of trace evidence examination in general; common polymers do not yield much information, with the exception of those containing vinyl chloride, silicone, heavy atoms such as bromine and sulphur, and certain aromatic rings. The work of Suzuki was carried out on the macroscopic scale because conventional IR microspectrometers cannot operate in the extended region. A 700 cm^{-1} is usually the lowest frequency that can be measured. Synchrotron IR microspectroscopy on the other hand offers the possibility for extended-range IR microspectroscopy of paints and other materials, thereby opening up new horizons in trace evidence analysis. The main limitation is spatial resolution, which would be of the order of 30 μm at 300 cm^{-1}, therefore the examination of very small flakes of paint or thin fibres would be compromised to some extent. Stich et al. [16], using a Raman microprobe, has indicated that vibrational spectroscopy is of use in the characterization of primer-derived GSR; carbonates, sulphates, and oxides of lead and barium were tentatively identified. Extended range synchrotron reflectance IR microspectroscopy might contribute more information regarding the composition of primer-derived residues.

The literature is silent as to whether synchrotron IR microspectroscopy offers any advantages over Raman microspectroscopy. Raman spectroscopy is subject to unpredictable, and sometimes intractable, problems due to background fluorescence. On the other hand, the probe beam used in Raman microspectroscopy can be brought into focus on a spot only a few microns in size. Scattering from a spot of this size can provide vibrational spectral data down to about 50 cm^{-1}. Infrared spectroscopy cannot match this spatial resolution performance, even with a synchrotron source, because of the wavelength of probe radiation lengthens into the near-IR, the diffraction limit applicable also increases. Raman therefore might be the technique of choice for the collection of extended range vibrational data at high spatial resolution for trace evidence. Raman microspectroscopy and IR microspectroscopy are best described as complementary techniques: each has something to offer the trace evidence analyst and can be used effectively in conjunction.

Synchrotron radiation is highly polarized; this has two implications for trace evidence examination: one a potential benefit; the other a caution. In relation to the former, IR dichroism offers an extension to IR spectroscopy as a means of within-class discrimination of those polymers that conform to a preferred molecular orientation. As a result of polymer chain orientation along the axis of the fibre, certain peaks in the IR spectrum of polyethyleneterephthalate (PET), for example, are strong or weak depending upon whether the polarization of the IR beam is oriented along the axis of the fibre or perpendicular to it. The ratios of the two extremes of peak areas are referred to as dichroic ratios. Of relevance to forensic science is that dichroic ratios depend upon the tension applied to the fibres as they are spun, and therefore to some extent are dependant upon the method of manufacture. Dichroic ratios therefore can be a means of discriminating fibres. As indicated by Cho et al. [17] and Tungol et al. [18], IR dichroic ratio analysis is a useful means of discriminating between PET fibres. Cho was able to classify 32 distinct PET fibres into 22 groups on the basis of their dichroic ratios, IR analysis alone allowed discrimination of only 13 groups. In another study, Cho et al. [19] demonstrated the forensic utility of IR dichroic measurements on acrylic and nylon textile fibres. Synchrotron IR microspectroscopy might have something to offer in relation to discrimination of materials on the basis of their dichroic ratios. Firstly, the high signal-to-noise capability will enhance peak area precision; this might allow better discrimination within the PET class. Secondly, better data reliability might allow subtle dichroic ratios to be measured in other fibre- or film-forming polymers of forensic interest, offering new means of discrimination. For example, Ellis et al. [20] has measured dichroic ratios in isotactic polypropylene using synchrotron IR microspectroscopy. As a cautionary note, unlike conventional IR microscopy, where one must intentionally polarize the beam in order to measure dichroic ratios, synchrotron IR microspectroscopy always involves a polarized beam. Therefore, at least in the case when fibres are examined, it would be good practice to ensure that the orientation of questioned and control fibres with respect to the beam remains constant in order to guard against type 1 errors arising from dichroism.

In summary, microspectrometers equipped with synchrotron sources offer greatly superior analytical capabilities in the mid-IR for specimens smaller than about 50 μm. Enhancements can be expected in relation to signal-to-noise ratio, which allows more reliable measurement of weak signals, and as a result of better diffraction characteristics, which allows better photometric accuracy and rejection of spectral leakage. Synchrotrons also offer the capability for extremely high resolution experiments, and the recording of spectral details of rapidly evolving chemical systems such as living cells. However, potential or real examples of applications of these capabilities to trace evidence examination are not evident. The ability to collect data rapidly at high signal-to-noise ratio makes synchrotron IR microspectroscopy the technique of choice for IR mapping experiments. The advent of focal plane array detectors coupled to synchrotron sources will also assist in this area. Although such a capability is not often required for case work, it might be of great use for research purposes.

4. X-ray absorption and fluorescence techniques

In this section we have included any technique that relies on the absorption of incident X-ray radiation to infer chemical information. However, absorption is often not measured directly. X-rays are impinged upon a sample and the associated absorption and interaction with the matter gives rise to the emission of photoelectrons, secondary electrons, Auger electrons and fluorescent X-rays.

X-ray absorption techniques offer many applications that relate to the characterization of materials. These can be in either solid, liquid or gas forms and hence experiments may be run in situ. Analyses can be performed with synchrotron techniques with sensitivities unsurpassed by conventional methods and can include bulk analysis or arranged to be surface sensitive.

While the increased brightness and tunability of synchrotron sources are offered as significant advantages for absorption, transmission and fluorescent techniques, there are other factors that additionally improve signal-to-noise. Scatter cross-sections are dependant on polarisation and exhibit a minimum in the plane of the synchrotron ring. Therefore, a detector placed in the same plane as the storage ring experiences less scatter then would be detected using a non-polarised beam (such as that generated from conventional sources). It is worthwhile to note that absorption cross-sections are not dependant on polarisation and hence sensitivity is not affected.

Perhaps the simplest concept utilising absorption and transmission of X-rays is micro-computed tomography (micro-CT). Beamlines have been developed that can provide incredible resolving power to produce “virtual cross-sections” in any plane of minute artefacts. At the APS, a high-throughput system has been described that provides data acquisition within minutes at anticipated resolutions on the order of 100 nm [21]. This technique can yield structural information of materials while being non-destructive. One area of application to forensic science is fundamental studies into the formation and/or structure of trace evidence. For example, fired Winchester 0.22 calibre ammunition gunshot residues (GSR) (Fig. 5), have been “cross-sectioned” by us to provide insight into their physical composition. In the example shown, the particle appears to be a conglomerate of low-density regions separated by a denser phase. While some of these low-density regions appear to contain material, others appear as though they are simply voids. The highly absorbing inclusions that appear white are condensed metallic spheroids. Scattering artefacts are observed in this example but can be reduced under optimised conditions. This preliminary example was generated at the 2-BM line at the X-ray Operations and Research Collaborative Access Team (XOR-CAT), APS, with a 16 keV incident beam and each pixel represents 1.3 μm × 1.3 μm. While analysis for the complete three-dimensional reconstruction of this particle required 1.5 h, under optimal conditions would have only required ∼15 min. The cross-sections produced by X-ray micro-tomography closely resemble those produced by Niewohner and Wenz [22], who used ion beams to physically cross-section particles. The intensity impinged upon a sample by conventional micro-CT instruments is extremely low and the associated bremsstrahlung radiation reduces monochromacy. However, the use of a synchrotron source results in high X-ray flux with very small beam divergence and a wide energy spectrum for selection of the most suitable energy for experiments [23–25]. Furthermore, the small divergence of synchrotron X-rays allows longer optical paths for imaging, thus reducing scattered radiation superimposition. Other imaging capabilities are also an area to benefit from the advantages of synchrotrons such as diffraction enhanced imaging at the Laboratório Nacional de Luz Síncrotron (LNLS, Brazil) [26], and radiography, tomography and diffraction topography at ESRF [27].

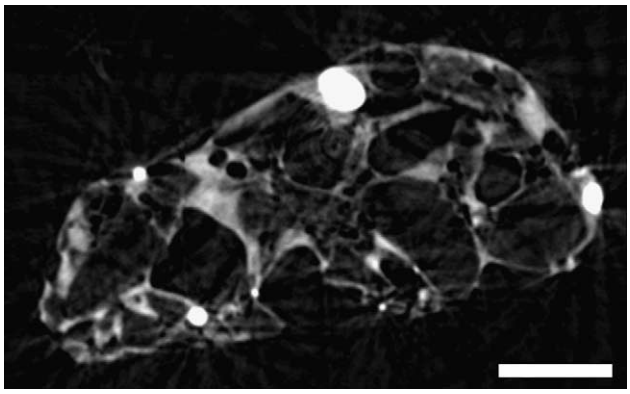

Fig. 5. An X-ray tomography ‘slice’ obtained from a glass containing gunshot residue particle. Bar = 100 μm.

Rather than purely physical properties, however, trace evidence analysis largely depends on chemical information, for

which synchrotrons offer a number of advantageous techniques that are the primary focus of this review.

There is a good general awareness and understanding of the mechanisms which common techniques such as IR spectroscopy, X-ray diffraction and fluorescence utilize. X-ray absorption fine structure (XAFS) techniques are less well known and are worthy of a brief description to increase familiarity. As X-rays pass through a material, a proportion of them will be absorbed. Measurements of the amount of absorption as a function of X-ray energy reveals edge structures where the level of absorption abruptly increases. The edge occurs when, with increasing energy, an incident photon has sufficient energy to cause the transition of an electron to an unfilled bound state, e.g. from an s-character to a p-character state.

A typical X-ray absorption spectrum is reproduced in Fig. 6. The absorption edge, which is essentially the X-ray absorption coefficient as a function of incident X-ray energy, is element specific and comprises electron transition and configuration information together with features that are modified by electron scattering with nearest neighbour atoms. An advantage of this technique is its usefulness in analysing a wide variety of solids and liquids, including dissolved species. High energy-resolution detectors also allow higher scrutiny of the XAFS features giving rise to techniques such as X-ray absorption near edge structure (XANES) and extended X-ray absorption fine structure (EXAFS) (Fig. 6). Examples of XAFS beamlines have been described at the ESRF [28], the National Synchrotron Radiation Laboratory (NSRL, China) [29] and the APS [30]. XANES is also sometimes referred to as near edge X-ray absorption fine structure (NEXAFS) by soft X-ray specialists. These techniques utilize fine features in the absorption spectrum, i.e. absorption versus energy. The absorption edge of a transition is the region at which the incident energy is sufficient to start interacting with the element under consideration and hence, is absorbed. Interpretation of X-ray absorption spectra commonly uses standard compounds with known structures and oxidation states, but can also be compared with theory to derive the structure of a material. Detection limits are usually in the low-ppm range and hence, in a forensic context, can be used to speciate trace elements within a sample.

The XANES region, comprising the absorption edge itself and the features immediately beyond the edge (to ∼50 eV after the edge) [31], are strongly sensitive to the oxidation state and co-ordination chemistry of the absorbing atom of interest. XANES spectra are commonly compared to standards to determine which species are present in an unknown sample. Once species are identified, their relative abundance is quantified using linear-combination fitting (or other curve-fitting algorithms) using XANES spectra of the standards to reconstruct the experimental data. It is important to note that XANES is sensitive to bonding environment as well as oxidation state. Consequently, XANES is capable of discriminating species of similar formal oxidation state but different co-ordination. For example, with the use of appropriate standards, the proportions of Fe(II) and Fe(III) in a material may be determined and whether Fe is octahedrally or tetrahedrally co-ordinated with sulphur or oxygen.

The EXAFS region comprises information on nearest neighbour distances and the particular ligand atoms. EXAFS comprise periodic undulations in the absorption spectrum that decay in intensity as the incident energy increases well past (∼1000 eV) the absorption edge. These undulations arise from the scattering of the emitted photoelectron spherical wave with the electrons of surrounding atoms. This process acts to modulate the absorption coefficient accordingly. Analysis of this part of the spectrum firstly involves background subtraction and normalization, and converting the photon energy scale to *k*-space units (wavenumbers, $Å^{-1}$). The Fourier transform of the normalized data yields a radial distribution series of maxima corresponding to the distance of successive shells of nearest neighbour atoms [1]. Fig. 7 illustrates the final treatment of the EXAFS portion of the Cu K-edge spectrum from Cu metal shown in Fig. 6. Alterna-

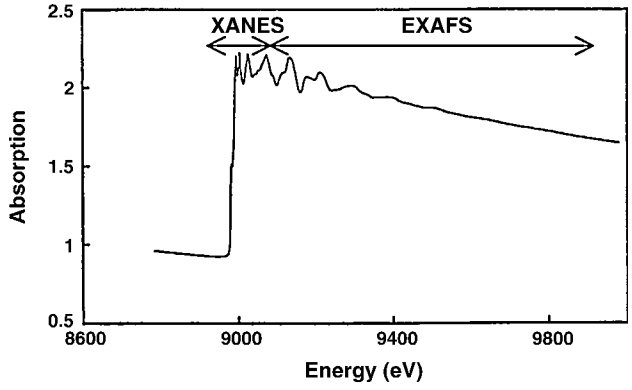

Fig. 6. An example of an XAFS spectrum obtained of the Cu K-edge from Cu metal highlighting the XANES and EXAFS regions. Reprinted, with permission, from [137], copyright by World Scientific Publishing Co. Pte. Ltd.

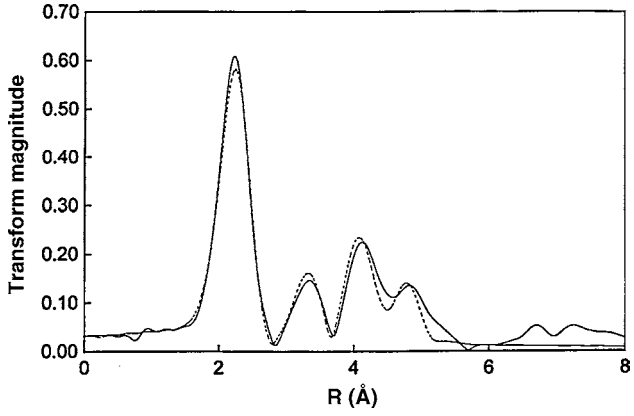

Fig. 7. A *R* (Å) plot for Cu metal derived from the Cu K-edge spectrum in Fig. 6 reveals radial distributions of the surrounding atomic shells. Computational modelling (dotted line) confirms the four atomic shells surrounding a central Cu atom in its metal form. Reprinted, with permission, from [137], copyright by World Scientific Publishing Co. Pte. Ltd.

tively, an EXAFS may be calculated from a proposed model structure using theoretical scattering models. The theoretical spectrum can then be matched to the experimental spectrum, confirming the identity, number and distance of neighbouring atoms [1,31].

Acquisition of data may be performed by a number of mechanisms. Transmission or absorption simply requires a detector positioned in line with the incident X-rays behind the sample. In the soft and intermediate energy X-ray regime (less than ∼3–4 keV), scanning transmission X-ray microscopy (STXM) lines such as those at the Advanced Light Source (ALS, USA) [32] and the National Synchrotron Light Source (NSLS, USA) [33] offer microscopic and spectroscopic analysis of low energy transitions including C-, N- and O-edges with NEXAFS capabilities [34]. These lines can often also provide analysis of the K-edges of the group 3 metals, and also the L- and M-edges of higher atomic number elements such as the 100–1500 eV line at the Laboratoire pour l'Utilization du Rayonnement Electromagnétique (LURE) [35]. Other soft X-ray spectroscopy experiments have been described at NSLS [36], and has also been combined with tomography [37]. However, soft energy experiments are complicated by a number of factors including severe absorption in air (particularly by Ar). Hence, such analysis should be conducted in a low-Z atmosphere such as He [38], or in vacuum. If organic components are not important, higher energies can be utilised with less instrumental and acquisition problems.

Hard X-ray (>3–4 keV) beamlines are employed for X-ray absorption spectroscopy (XAS) measurements for elements of atomic number above potassium as those elements with lower atomic number do not have electrons (i.e. K, L, M, etc. transitions) with binding energies in this range. However, hard XAS may be performed in air, outside the vacuum of the beamline, via an X-ray transparent window. This reduces the need for vacuum-safe sample preparation and enables XAS of liquids and suspensions.

Alternatively fluorescence yield or electron yield may be measured. Fluorescence and electron emission result from de-excitation processes occurring after absorption. Fluorescence yield (FY) and total electron yield (TEY) measurements, as they are called, can be made simultaneously, FY using a semiconductor X-ray detector and TEY by monitoring the sample drain current with a high precision current meter. X-ray fluorescence can be measured in a position on the incident beam side of the sample. The excited volume is represented by a depth approximately equal to the X-ray attenuation length. The re-emission of the fluorescent X-rays can be detected and used to produce a fluorescence spectrum or analysed to give an absorption-based analysis. Combining FY and TEY measurements yields both bulk (few thousand Angstroms) and near-surface (few tens of Angstroms) information, respectively, due to the shallow escape depths of the emitted secondary electrons contributing to the drain current. A further variant is partial electron yield (PEY), which involves the energy-selective detection of emitted photoelectrons or Auger electrons [31].

4.1. Synchrotron X-ray fluorescence (SXRF)

Several conventional techniques are available to the trace evidence examiner for the purpose of trace element profiling and bulk analysis; this section compares the performance of these techniques with SXRF. Perhaps the most commonly available technique is scanning electron microscopy-energy dispersive X-ray microanalysis (SEM-EDX). Although this technique can be use for the analysis of bulk materials (e.g. window glass [48]), its detection limits preclude its utilization as a tool for trace element profiling. Conventional X-ray fluorescence finds some use in trace evidence examination. For example, Howden et al. [39] used energy dispersive X-ray fluorescence for distinguishing sheet glass from container glass. A similar approach was taken by Ryland [40] who employed energy dispersive X-ray fluorescence (ED-XRF) to classify glass types (i.e. sheet or container) by elemental composition. Koons et al. [41] performed a comparison between refractive index (RI), ED-XRF and inductively coupled plasma atomic emission spectrometry (ICP-AES) in their application to forensic characterization of sheet glass fragments. More recently, Kunicki-Goldfinger et al. [42] employed radioisotope ED-XRF in provenance studies of glass originating from 18th century glasshouses in Central Europe. Becker et al. [43] and Hicks et al. [44] also utilised energy dispersive X-ray microfluorescence for the classification and discrimination of glass. Other highly sensitive analytical techniques, which also find application within forensic science, include time-of-flight secondary ion mass spectrometry (ToF-SIMS) and laser ablation inductively couples plasma mass spectrometry (LA-ICP-MS). Both techniques offer the ability to obtain trace element and isotopic ratio data for a wide variety of trace evidence, including glass, gunshot residues and inks. Becker and Stoecklein [45] demonstrated that elemental analysis of glass fragments by LA-ICP-MS was a rapid screening technique to differentiate between different glass types. Almirall [46] and Trejos et al. [47] have applied LA-ICP-MS for the elemental characterization of glass while Watling [48,49] additionally analysed metallic residues resulting from safes, firearms and construction material. The technique has also been applied to the fingerprinting of gold deposits and gold products in South Africa [50] and the provenance establishment of gold and diamonds in Western Australia [51]. By comparison of elemental composition, such minerals can be related back to a specific mineralizing event, mine, and country of origin. Advantages offered by LA-ICP-MS include short analysis times, little sample preparation, high precision (<10%) and accuracy, and excellent detection limits (sub picogram levels) [47]. The technique is said to be non-destructive, however data presented by Trejos et al. [47] indicate that under typical acquisition parameters, an ablation crater of approximately 50 μm results. Furthermore, despite the capability for spatial resolution down to 10 μm, Almirall and Furton [52] found that better reproducibility is obtained when operating at 50 μm. This therefore limits the allowable sample size to greater than 50 μm and may result in significant destruction

of small samples. ToF-SIMS on the other hand, is a highly surface sensitive (first one to two monolayers) technique that can provide chemical as well as elemental information with much less destruction of the sample. Compared to LA-ICP-MS and ToF-SIMS, SXRF offers equivalent or better limits of detection together with no sample destruction.

Conventional X-ray tubes for XRF experiments are limited by the ability of the X-ray source material to dissipate heat generated from the impacting electron beam used to generate the X-rays. Collimation and focusing of conventional sources for microanalytical techniques also leads to a severe reduction in transmitted flux due to the lack of directionality in their emission. Synchrotron X-rays are generated with a naturally low divergence and hence the production of a micro-analytical beam does not suffer from the same degradation. An early assessment of synchrotron micro-XRF compared to conventional XRF has been made from the mid- to late-1990s [53]. While this publication highlights the advantages of synchrotron XRF over conventional methods, it is also of interest to compare how far the synchrotron techniques have developed in recent years. The sensitivity of synchrotron X-ray fluorescence offers a technique that is non-destructive and can measure trace quantities with unsurpassed sensitivity. This enables profiling material based on trace elemental composition that can reflect origins or identify evidence as originating from the same, or different sources. “Impurity profiling” can be done more sensitively on smaller samples than alternative techniques while being non-destructive and with no, or very little, sample preparation.

Synchrotron XRF applied to forensic or similar samples is limited, but active, and has been applied in art and archaeometry contexts [54]. The latter, studied and classified various ancient glasses as well as presenting other interesting case studies involving ink analysis and weathering effects on glass and coins. These types of cases typically explore questions similar to forensic investigations such as aging effects, localizing origins of artefacts and identifying composition, but similarly have not appeared in a significant number of synchrotron orientated publications.

Muratsu et al. [55] used synchrotron radiation total reflection X-ray fluorescence (TXRF) spectroscopy (incident angle of 0.005°) to detect trace elements in small amounts (10 μg) of drugs (methamphetamine, amphetamine, 3,4-methylenedioxymethamphetamine, cocaine, and heroin) in order to discriminate sources and synthetic routes of manufacture. Data acquired from methamphetamine from synchrotron and conventional sources has been reproduced in Fig. 8. They report on measuring quantities down to 10 pg with accumulation times of 500 s. Accumulations of 1000 s by conventional TXRF could not detect iodine or iron in the example shown. It would therefore appear possible to use SXRF for the elemental profiling of single crystals of drug within a “cut” specimen. This would allow comparison of seizures to take place without the confusing issue of the cutting agent contributing to the elemental profile. In addition, trace botanical samples, i.e. marijuana and opium, were also analysed for discrimination.

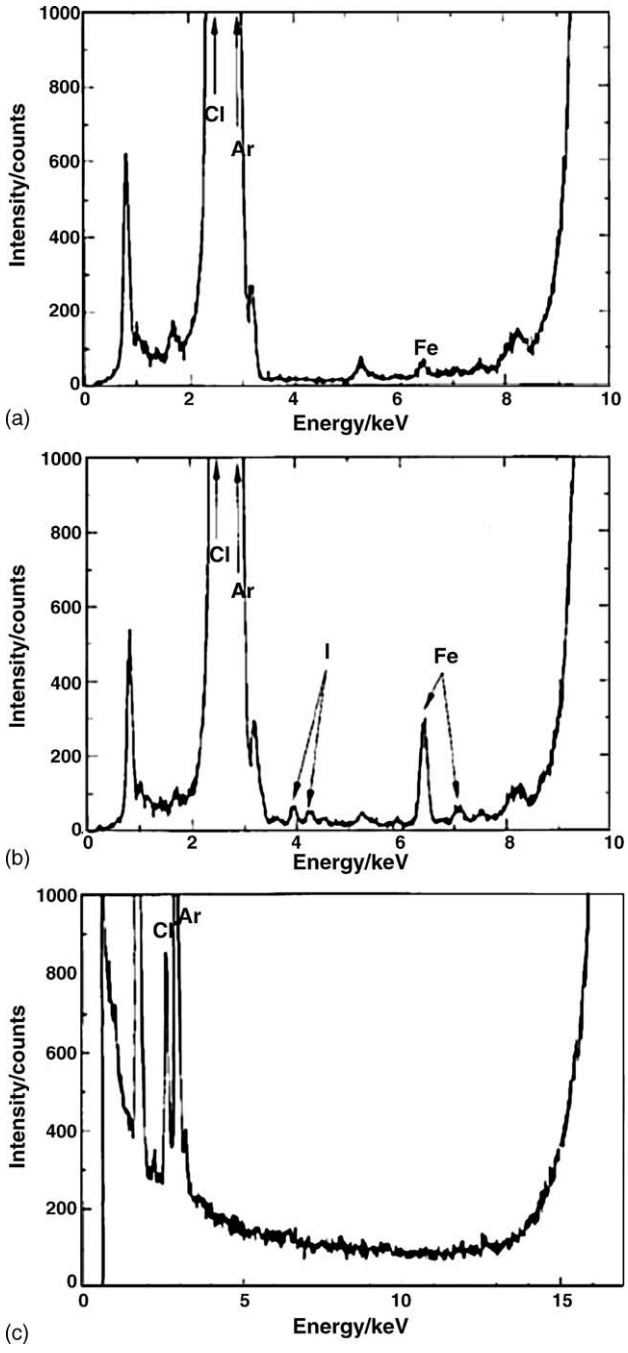

Fig. 8. Impurity profiling. Synchrotron TXRF spectra from a control methamphetamine HCl (a), a seized methamphetamine HCl (b), and a conventional TXRF spectrum from the same seized sample (c). Reprinted, with permission, from J. Forensic Sci. 47 (5), copyright ASTM International, West Conshohocken, PA 19428.

An additional advantage of using a synchrotron source is the tunability of the incident X-ray energy. In some cases, a specimen may contain elements that produce overlapping X-ray fluorescence peaks, for example the As-K and Pb-Lα emission lines. Since for Pb, the fluorescence is generated from an L transition, more energy is required to remove the inner shell electron than what is required for the As inner

shell electron. Therefore, the incident energy can be tuned to a point above that required to remove the As electron, but insufficient for the Pb-Lα transition to occur. Therefore, the presence of both of these elements can be confirmed. Note that Pb-Lβ can still be utilised for a unique Pb signal.

Anjos et al. [56] employed total reflection X-ray fluorescence using a polychromatic synchrotron radiation source for quantitative trace elemental determination in red and white wines, indicating application for quality control operations. The same technique was applied by Costa et al. [57] for the elemental analysis of mineral water. Detection limits were quoted in the low-ppm range and the accuracy of the technique was determined to be 4% [57]. This work also demonstrated the ability to determine the origin of the mineral water and wines based on elemental composition.

A relatively high profile investigation that has utilised synchrotron radiation was that in which four people died after consuming poisoned curry dosed with arsenic at a festival in Japan. Suzuki et al. [58] used SXRF in an attempt to discriminate 13 samples of arseneous acid based on heavy metal content due to origin and manufacturing method. By this analysis they were able to profile arseneous acid from a selection of sources including samples obtained from a suspect's home. An exciting energy of 115 keV was used to analyse for K-α lines to avoid interferences of lighter elements. Nakai et al. [59] also showed the use of high energy exciting radiation (116 keV) for the detection of rare-earth (all at 50 ppm concentrations) and heavy metals in standard rock and glass samples. The best detection limits obtained were 0.1 ppm for W after 500 s acquisitions. The estimated minimum detection limit for Lu (as an example of rare-earth elements) was 16 pg. This data demonstrates the potential of synchrotron XRF analysis to be used for the profiling of various materials.

Suzuki et al. [60] has used SXRF for the determination of the elemental content in car headlight glasses. Significant differences were measured non-destructively in several trace elemental concentrations to discriminate between samples with less than 0.5 mg of material. Confocal SXRF was used by Smit et al. [61] for the elemental analysis of paint layers. In confocal SXRF a two-lens system is used for focussing the irradiating beam and the fluorescence detection to a common volume. Only elements within this volume yield a fluorescence signal that is detected. The beam control is such that the excitation volume can be arranged to be within the specimen at a user-defined depth. Depth profiling can therefore be achieved without the specimen being sectioned, as is usually required with conventional techniques such as SEM-EDX or XRF. The analysis by Smit et al. [61] on multilayer car paints achieved a depth resolution of 30 μm, quite sufficient for determining composition and thickness of the paint layers. Apart from the obvious advantage that confocal SXRF does not require the sectioning of specimens, it also allows the operator to analyse the specimen in a region beneath any surface contamination.

It is not unusual for synchrotron XRF experiments to quote fluxes much greater than 10^{10} photons/s focused into micron sized spots. When discussing such large impinging fluxes, concern arises regarding any detrimental effects of the analysis on the sample [62–64]. Radiation damage has been shown to be a problem, especially with, but not limited to, organic samples [65–67]. While damage can readily alter or even destroy a sample, precautionary approaches in sample preparation or sample conditions during analysis can minimize any risk of sample degradation or alteration. While flux, beam size, or analysis time can be reduced (to the detriment of the experiment) to help prolong sample integrity, other options are also available which do not inhibit sensitivity, such as minimizing water content and using streams of cryogenic gases [68]. However, under appropriate conditions for more robust samples, analysis is truly non-destructive. Kempenaers et al. [69] conducted 300 replicate XRF analyses upon a single 5 μm × 8 μm region within a 1 mm thick wafer of glass (NIST SRM 613) and concluded that there was no sign of material degradation or loss of analyte throughout the experiment.

Quantification is an important issue especially when it is desirable to compare results or develop methodologies against other well-established techniques that provide quantified data. Quantification is available from synchrotron analysis and becomes easier when considering monochromatic beams since matrix effects are easier to describe. However, to apply synchrotron XRF to more novel applications various analytical complications are encountered, but can still be accounted for, for instance in analyses of inclusions [70], uncommon materials, soft X-ray transitions or on microscales [71].

Kawai et al. [72] studied fly-ash particles with TEY for surface sensitivity and FY for bulk data. The results indicated surface concentration differences in Pb between sources of fly-ash particles from incinerators. Soft X-rays were used for excitation of the S K-edge and the Pb M_4- and Pb M_5-edges in vacuum at 10^{-6} Torr. They propose that the Pb in the higher temperature incinerator (1600 K) vaporizes and subsequently condenses onto the surface of the fly-ash particles when cooled. These samples are somewhat analogous to GSR particles, in that they are small particles that experience high temperatures in oxidizing environments containing vaporized metals. Conventional techniques have also been applied to the characterization of GSR and again, highlight an area in which fundamental research by synchrotron methods could be applied. Charpentier and Desrochers [73] used conventional micro-XRF to analyse lead free primer-derived GSR while Brazeau and Wong [74] used micro-XRF for the analysis of GSR on human tissue and clothing. An evaluation of micro-XRF on the elemental analysis of GSR was performed by Flynn et al. [75]. It was found that a disadvantage of the technique using a 100 μm beam collimator was the inability to analyse particles smaller that 10 μm, a feat easily achievable with a synchrotron source. Vincze [76] developed a Monte Carlo simulation based approach to quantify trace

elemental levels in individual micrometer sized fly-ash particles. SXRF analysis was performed with 300 s live time counting and improved detection limits up to roughly two orders of magnitude better than conventional systems.

Rindby et al. [77] also used micro-XRF to analyse large fly-ash particles with a 13 keV 2.3 μm full beam with 10^{10} photons/μm^2/s and an energy bandwidth of $10^{-4}\Delta E/E$. In their arrangement, concentrations were measured down to ~200 ppb for Zn and Cu in a few seconds corresponding to about 10^{-16} g of material for thin samples. This enabled analysis of particles between 20 and 40 μm in diameter and even composition and homogeneity of sub-particles with submicron diameters within the larger particles.

The use of synchrotron XRF for environmental monitoring was demonstrated by Ide-Ektessabi et al. [78]. In their study the elemental composition of teeth was measured to indicate environmental exposure such as heavy metal contamination. Similarly, Anjos et al. [79] performed elemental mapping of teeth using synchrotron micro-XRF. Teeth are excellent indicators of environmental exposure as elements are sequestered by the mineral phase of teeth during their formation. Advantages of SXRF for such applications include its non-destructive nature and simple sample preparation. The beam size in this study was 7 μm × 6 μm allowing high spatial resolution, and the high-collimation of the synchrotron source permits high efficiency for trace element determination [80]. These advantages enhance the applicability of SXRF for forensic material discrimination based on elemental analysis. Although it has been shown that trace-elemental analysis of hair for general diagnostic analysis of many elements is highly questionable [10,80,81], and even washing procedures can produce misleading results, there still remains potential for the detection of ingested metals that may occur in large doses and that are unlikely to be due to external contamination. Individual hairs may be analysed longitudinally and non-destructively by XRF to reveal ingestion of toxic metals that may indicate poisoning. Toribara [82] used conventional XRF to longitudinally analyse a hair from a woman who experienced mercury poisoning and showed the point of ingestion and subsequent diminishing concentration with time. Nicolis et al. [83] also demonstrated longitudinal temporal variations. They used SXRF to show fluctuations of As in hair due to a period of use of an As-based drug used for the treatment of leukaemia. These examples demonstrate the potential to use hair as a monitor to allocate a time designation to a period of exposure to toxic metals. In addition to this however, chemical variability in hair can also be indicated by XRF measurements. Bertrand et al. [84] studied hair from Egyptian mummies with synchrotron techniques. Small angle XRD confirmed retention of structural integrity of the keratin with a beam size down to 5 μm. IR analysis was also performed to analyse protein secondary structure and SXRF analysis revealed cross-sectional distributions, which suggested the detection of embalming and cosmetic treatments. This work could be extended to identifying elemental components of hair treatment products for comparison of individual samples. Soft biological matrices can also be analysed, for example breast tissue Geraki et al. [85] and brain sections Liu et al. [86].

In addition to highly sensitive XRF data for trace-elemental information, synchrotron XRF is a highly useful mapping tool for high resolution imaging. Examples of high resolution images obtained at the X-ray Operations and Research Collaborative Access Team (XOR-CAT) 2-ID-D beamline (APS, USA) are given in Fig. 9. The images portray a 2 μm thick transverse slice of hair that was scanned with a 13.1 keV 100 nm spot and a dwell time of 2 s per pixel. The S (originating from the keratinous protein) reflects the hair sample, while Cu and Pb images indicate localizations of metal concentrations around the cuticle edge and what are likely to be melanin granules or nuclear remnants of the cortical cells. These images portray the highly detailed spatially resolved information that a synchrotron beam can produce which can be useful for describing minute samples.

The above examples highlight the advantageous characteristics of synchrotron XRF, which include its non-destructive nature, monochromaticity, ability for simultaneous determination of multi-elements, high-sensitivity, small sampling volume and effectiveness for microanalysis.

4.2. X-ray absorption near edge structure (XANES)

While SXRF can provide a highly sensitive method for determining composition, analysis of the X-ray absorption edges can provide additional information regarding the chemistry of individual elements. XANES analysis utilises edge features that reveal the short-range order of the environment surrounding atoms of an element of interest. This information can yield data that could be used as an additional discriminating tool for material characterization. This method offers significant potential in a forensic context.

Near edge spectral variations are strongly dependent on the electronic configuration and its interplay with the atomic structure. These features provide information on the local surroundings of absorbing atoms such as valency, chemical environment, coordination geometry, effective charge and symmetry of unoccupied electronic states. Typically, XANES analysis will include a variety of standard materials that are well characterized to infer properties of the local environment. XANES analysis can be performed with beams of the same dimensions as those used for SXRF, i.e. down to spot sizes on the order of tens of nm.

Structural information can be obtained from the high energy-resolution analysis of absorption edges or the XANES region. The spectral features are a linear convolution of the relative contributions due to each of the oxidation states present. With proper analysis, quantitative information can be extracted regarding the contribution of each oxidation state. This has been demonstrated in glass [87], minerals [88] and even glass inclusions [89]. While an elemental concentration can be the same between samples, relative abundances

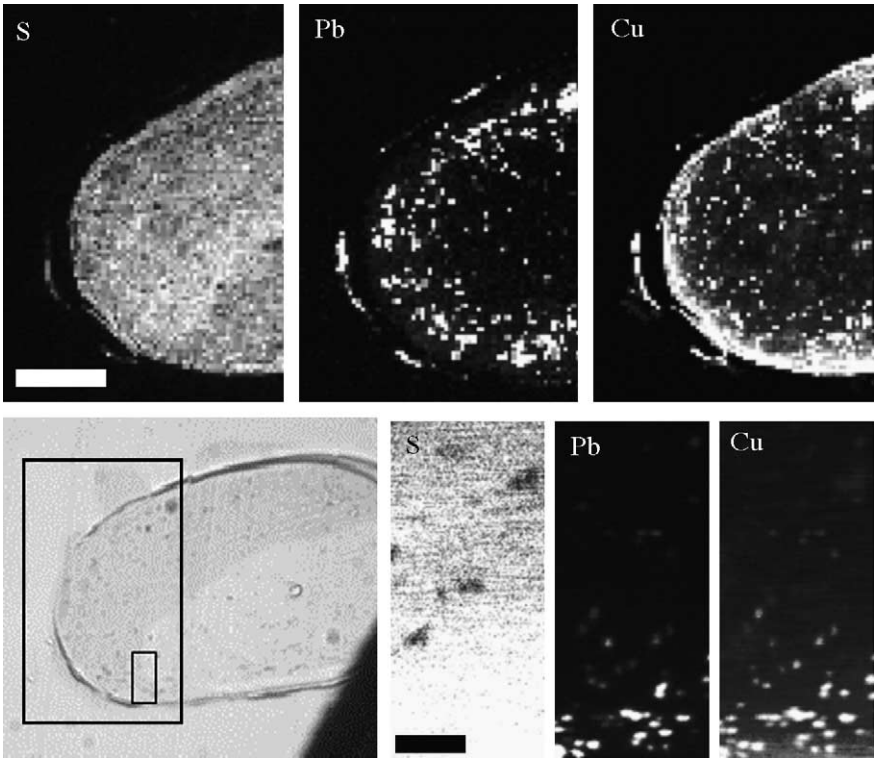

Fig. 9. Synchrotron XRF mapping of a 2 μm thick hair section. The optical micrograph indicates the areas over which elemental maps were produced with a 100 nm spot size and 2 s dwell time per pixel. The bar = 10 and 2 μm for the larger and smaller images, respectively.

in oxidation states can be different providing an additional degree of discrimination. The data can reflect environmental conditions during the formation of a substance, for instance the formation of volcanic glasses, from which the oxidation states present are used to infer redox conditions at formation. This information has obvious potential to be extended into forensic work to identify or discriminate manufacture methods of materials or the conditions under which evidence has been generated.

Typical XANES analysis of particulate matter may be extended to an additional discriminating factor for particles obtained as trace evidence such as soil, glass and GSR. In the case of GSR there is application in studying the content and chemistry of the resulting particles. Understanding the effect of discharge on trace-elemental concentrations and the oxidation state and coordination of those species can help to relate or discriminate fired and unfired ammunition and differences between ammunition or firearms. In addition, particles may conclusively be discriminated from environmental particles. SEM-EDX is the most common technique for GSR analysis, which has a depth resolution of approximately 1 μm. Hellmiss et al. [90] applied Auger electron spectroscopy (AES) to the analysis of GSR with a greater surface sensitivity, generating data that originates from the uppermost atomic layers (0.3–3 nm). AES is not limited to surface analysis however, and can be used simultaneously with ion sputter etching to allow depth profiling. Unlike SEM-EDX equipped with windowed X-ray detectors, AES has the ability to detect elements of low atomic number. The study by Hellmiss provided some insight into the complex internal composition of GSR particles. AES was also applied by Zeichner et al. [91] to study the surface concentrations of antimony (0.5–3%, w/w) in hardened lead projectiles. ToF-SIMS has also been applied to gunshot residue analysis [92,93] where it was determined that the elements present in GSR are not simply in elemental form but form compounds such as oxides and hydroxides. Furthermore, the presence of glass in several types of 0.22 calibre ammunition was ascertained. Elemental analysis by ToF-SIMS allowed characterization of the glass present and the linking of residues with putative source ammunition. Synchrotron analysis (XRF, XANES, AES, etc.) however, can detect all elemental constituents in a completely non-destructive manner, with or without surface sensitivity, with the added benefit of deducing elemental oxidation states and coordinations. Examples of Fe K-edge XANES spectra are provided in Fig. 10 which were acquired at the Australian National Beamline Facility at the Photon Factory (Japan). Several spectra from standard materials are included along with data recorded from a group of glass-containing GSR. The XANES spectrum from the GSR appears to be a convolution of different chemical forms. A significant proportion resembles the spectrum of iron metal, while comparison with Fe compounds presented by Westre et al. [94], indicates the possibility of an octahedral Fe^{III} complex. Other oxides or

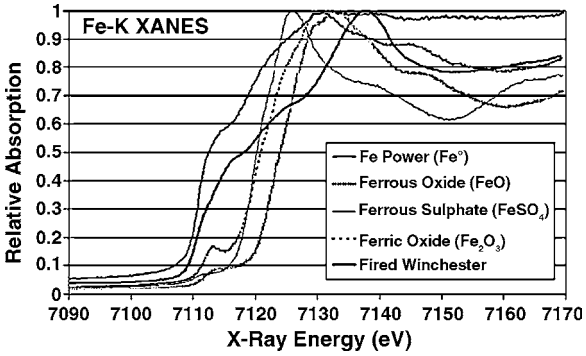

Fig. 10. Fe-K XANES spectra from a variety of iron containing compounds. The spectrum of the iron content in the GSR particles indicates similarities to a combination of iron metal and a higher coordination phase.

iron sulphate do not appear to have contributed in any significance.

The low energy photoelectrons produce analysis of a surface sensitive nature, which can also be utilised for the XANES technique. Kawai [95] have shown that S (0.1–0.3%) exists differently in the bulk and surface of fly-ash powders (70% of particles had diameters less than 5 μm) with simultaneous total electron yield and XRF measurements. The bulk and surface S composition were characterized. The outer surface exhibited S^{6+} while the core was a mixture of S^{2-} and S^{6+}. They also indicated that the ratio of the oxidation states varied depending on the sources of coal, and hence this information has potential in discriminating such samples [96].

Fe oxidation state ratios have received the focus of many XANES studies [94], especially in glasses [97]. It follows that XANES analysis could extend itself to forensic discrimination of glass. The glass industry has demonstrated application in analysis of the depth dependence on the Sn, Fe and S oxidation states in float glass [98]. In addition to analysis of Fe^{2+} and Fe^{3+} ratios in glass, they have also been examined in historic inks [99]. Work of Coumbaros using ToF-SIMS demonstrates the presence of various inorganic elements as well as the organic dyes [100]. It follows that there is scope to enhance discrimination using XANES for these components. Here, XANES analysis could be applied to identifying the source of inks as well as studying alteration of both organic and inorganic components over time.

The amount of materials research available that utilise XANES analysis demonstrates this as a powerful technique for understanding the chemistry of compositional elements. Although there are not many examples of XANES analyses applied to forensic samples, there is the potential of such measurements providing an additional degree of characterization. It is unlikely that XANES will add value to analysis of those types of evidence that yield highly discriminating multi-trace element profiles, it would appear to be of greatest utility where only a few elements are present. A case in point is GSR, where elemental ratios are highly variable between particles from the same source.

4.3. Extended X-ray absorption fine structure (EXAFS)

High resolution analysis of absorption effects can additionally produce EXAFS spectra which extends approximately 1000 eV above the absorption edge for an elemental transition. The information extracted from such spectra provides medium range order, giving type of ligating atoms and very accurate metal–ligand distances, but little information regarding coordination and active site geometry. Sample preparation is minimal and does not require complicating extraction, dissolution or concentration procedures.

Huggins et al. [101] performed XAFS analysis of S, Cl, V, Cr, Cu, Zn, As, Br, Cd and Pb as well as Mossbauer analysis for Fe on NIST particulate matter SRMs 1648 and 1650. This work demonstrates the ability to identify the speciation of each element and produce a highly detailed description of the composition of a material. A major conclusion indicated that differences in EXAFS data could be used as characteristic signatures to source particulate matter. This is rather more intensive analysis than XANES but is somewhat more rewarding in characterizing samples, in particular when analysed in parallel. Relative changes in coordination number between samples of borate glasses with equal elemental (samarium) concentrations has been shown from XAFS spectra [102]. Other highly detailed studies have been reported where the metal contents of contaminated soils have been characterized [103,104]. While elemental compositions can reflect a site of origin of soil material, the manner in which metals are incorporated is highly variable and reflect other chemical information regarding the origins, e.g. pH, which may not be able to be measured from trace evidence. Metals in soils are bound in different forms depending on the characteristics of the bulk soil properties such as pH [105] and the amount of organic matter [106].

To make EXAFS analysis more powerful, acquisition of X-ray diffraction data can often be acquired on the same beamlines and hence from identical positions used for generating EXAFS spectra [107]. This can provide a highly detailed reconstruction of the composition of materials that is not available from any other instrumental setup. A comprehensive review of synchrotron techniques applied to geological samples has been given elsewhere [108] including X-ray absorption, diffraction and fluorescence studies to characterize geological samples.

5. X-ray diffraction (XRD) and scattering

Conventional XRD has been used to characterize GSR particles [109] and, soils and rocks [110]. Rendle [111] has recently reviewed conventional XRD in forensic science. XRD is useful in the identification of mineral composition; however, data collection can be time consuming. Synchrotron XRD alleviates this issue, and has the additional ability of providing 2D diffraction patterns. Furthermore, the application of synchrotron micro-beam techniques

allows for localised analysis. Broekmans et al. [112] investigated the application of synchrotron radiation XRD for the analysis of ancient (third millennium BC) cooking pottery. Data regarding the pottery's mineralogy was used to make inferences concerning pottery technology (i.e. clay preparation and firing techniques). Synchrotron XRD was also used by Dooryhee et al. [113] for the analysis of art and archaeological material in order to associate them with a possible source, their provenance and means of manufacture. Hard X-ray microprobe beamlines often have capabilities to perform combined XRF mapping and spectroscopy with micro-XRD [114]. Powder diffraction experiments performed with synchrotron sources are also very rapid and sensitive [115,116]. Other interesting reports include high resolution experiments at SPring-8 [117] and time-resolved experiments at the ESRF [118]. Others have described microdiffraction of protein crystals at the ESRF [119] and single crystals at the APS [120]. diffraction anomalous fine-structure (DAFS) [121] and protein crystallography by single and multiple anomalous diffraction (SAD/MAD) [122,123] are also beneficiary techniques. Systems designed for diffraction experiments are becoming highly automated [124,125] with high throughput [126]. Some beamlines have become very versatile such as at the SRS where in addition to offering combined XRD and XAS, small- and wide-angle X-ray scattering (SAXS/WAXS) are also offered on the one line [127]. SAX can be applied to the analysis of microstructural features in the 10–1000 Å domain and is often applied to characterising size, shape and orientation of polymers and other materials. WAX is typically performed in conjunction, which provides information on a much smaller scale similar to XRD Other examples of scattering experiment beamlines include high energy diffuse scattering at the APS [128] and inelastic X-ray scattering at LNLS [129]. An interesting study by Hiller et al. [130] used SAXS to investigate heating effects on bone mineralisation, recognising the forensic and archaeological applications. These techniques would also be useful in characterising the composition of GSR.

While capabilities regarding spatial resolution have not been exhibited, the combined analysis of a microprobe for XRF, XAFS analysis and XRD experiments have been demonstrated to be a compilation of techniques providing incredibly detailed compositional and structural information with sensitivity and selectivity not possible without the use of a synchrotron source. Such papers demonstrate the ability to characterize materials in high detail with high spatial resolution.

6. Microheterogeneity studies

With the increase in spatial resolution, microheterogeneity needs to be considered when trying to infer bulk properties based on a technique which, although sensitive, is also highly localised. If a property is measured in a randomly chosen volume of a sample it is desirable that any subsequent analyses from other volumes returns the same result within the error of the instrument, i.e. the measurement is representative of the bulk property. As the analysis volume is decreased, it becomes more probable that fluctuations in the property will arise from inhomogeneity. At some point, while the instrument is still capable of an accurate measurement, the error between alternative analysis volumes has increased beyond the instrument error. To understand what the minimum size of a useful piece of evidence is, it is necessary to find the limit at which the real error between different volumes of the same sample exceeds, by an unacceptable amount, the instrumental error. What is of interest is to find the ultimate limit of distinguishability, i.e. what is the smallest useful piece of trace evidence that can be used for the purpose of reliable comparison with its putative source or other related pieces of evidence? Although statistics can be used to average over many sample volumes, in microscopic pieces of material there might not be sufficient amount of sample to obtain such statistics.

Microheterogeneity is likely to be dependant on many factors and vary between samples, materials and also on the actual property being measured. Although a sample can be broken down into smaller pieces until the limit due to heterogeneity is deduced, it is impossible to say that one fragment from another sample is also limited by the same volume requirement for homogeneity. However, understanding typical limitations can offer valuable assistance in adding confidence to the value placed on individual measurements from low sample numbers of minute evidence if other samples of similar origin have been well characterized. Alternatively, it might give some indication to the number of minute particles required for an average to be derived that is representative of the bulk material.

It is therefore necessary to clearly define the errors obtained due to the experiment and real fluctuations in concentration. This has been demonstrated by Kempenaers et al. [69,131,132]. The former publication discusses various approaches, causes and descriptions of heterogenous measurements, and specifically discusses obtaining the critical mass required for analysis to represent a homogenous sample by SXRF. Of most interest is the work that used micro-XRF as a means of describing the microheterogeneity of NIST SRM 613 (trace-elements in 1 mm glass wafers), a glass reference material. An X-ray beam of 5 μm × 8 μm was used to interrogate the NIST glass wafer at 441 positions (a 21 × 21 grid pattern) and intra- and inter-regional variances in the XRF intensities for many elements were measured. In this way the minimum mass of glass analytically representative of the entire specimen was estimated to be 0.1 μg for certain trace elements (Ni, Cu, Zn, Ga, Ge, Se, Rb, Sr, Y, Nb, Mo and Pb). At a later point [69], similar analysis of NIST SRM 613 was presented. In this subsequent publication, a Monte Carlo model was used to assist in the study heterogeneity. For a particle to appear homogenous for all of the elements measured in that study, a sample mass of at least 100 ng was suggested. Assuming a density equal to that of

SiO_2 (2.6 g cm^{-3}), then this would relate to a spherical particle with a radius of ~21 μm. However, other elements such as Se only require 1 ng (or roughly a sphere of 4.5 μm radius). NIST SRM 610–617 glasses are commonly used for elemental analysis. LA-ICP-MS analysis of these standards by Eggins and Shelley [133] revealed that all the standards had regions where at least 25 elements were either depleted or enriched. Additional standards that are being employed for LA-ICP-MS are the Schott manufactured float glass standards FGS1 and FGS2 [46], which are also currently being assessed by us using ToF-SIMS. Ongoing work by us has demonstrated that tin penetrates into both the float and non-float surfaces with concomitant depletion of certain elements within the glass.

In addition to variability in concentration, microheterogeneity may also influence chemical features. Cho et al. [17] observed variability between fibres from the same source relating to microheterogeneity using IR analysis. EXAFS can also be used to study heterogeneity of speciation of metals. Sulphur species have been found to be inhomogenous in soils. Sulphur compounds were quantified in bulk samples as well as individual particles at hundreds of nm resolution [134].

Understanding microheterogeniety in trace evidence is vital to enable confident discrimination and characterization of samples and determining adequate sample size. Microprobe synchrotron techniques offer the characteristics of a highly sensitive, localised and non-destructive analysis that enable detailed studies in this area of research and will enable the determination of such limits.

7. Summary

Obviously the extremely high-cost of synchrotron sources preclude their utilization in routine forensic investigations. However, a substantial number of countries have invested in national synchrotron facilities, opening up the possibility that synchrotrons could be used on an as needed basis when conventional analysis and case significance indicate that further discrimination power is both possible and warranted. Another major use of synchrotrons is in relation to fundamental research into the nature of materials commonly encountered in forensic casework, particularly trace evidence. Such research underpins and advances the art of casework by indicating new points of discrimination of specimens, and new means for establishing associations between specimens. For example, although gunshot residues have been analysed by forensic scientists for many decades, the exact composition of primer-derived residues is not really well described. Sophisticated new techniques are required to shed more light onto the exact chemistry of primer-derived GSR in order to identify whether there is more scope than is currently thought for the discrimination of primer GSR from GSR-like environmental particles, such as those described by Torre et al. [135]. As described by Romolo and Margot [136] and Coumbaros et al. [92], respectively, there is a need and a potential for linking GSR with putative source ammunition; synchrotron-based techniques have the capability to provide valuable information. Substantial work has been devoted to the exploration of elemental profiling as a means of comparing glass specimens, but at what size does a microscopic particle no longer represent the bulk glass composition, and how close to the float surface does the composition represent the bulk?

Compared to conventional techniques, synchrotron techniques are capable of providing the highest level of characterization in a non-destructive manner. Due to a relatively recent advent of the most powerful techniques, the potential characterizing power achievable in the near future promises to be an exciting time for taking trace evidence analysis to limits not seen before.

Acknowledgements

This work was supported by the Australian Synchrotron Research Program, which is funded by the Commonwealth of Australia under the Major National Research Facilities Program. Part of this work was performed at the Australian National Beamline Facility, also supported by the Australian Synchrotron Research Program. Use of the Advanced Photon Source was supported by the U.S. Department of Energy, Office of Science, Basic Energy Sciences, under Contract No. W-31-109-Eng-38. Argonne National Laboratory is operated by The University of Chicago under contract with the U.S. Department of Energy, Office of Science. The authors also wish to thank Francesco De Carlo, Cathy Harland, Garry Foran and Barry Lai for their assistance in acquiring the results presented here. The assistance of Richard Garrett and Gerry Roe was also appreciated.

References

[1] Synchrotron Radiation: Earth, Environmental and Material Sciences Applications. Short Course Series 30, Mineralogical Association of Canada, 2002.
[2] G.L. Carr, J.A. Reffner, G.P. Williams, Rev. Sci. Instrum. 66 (1995) 1490–1492.
[3] J.A. Reffner, P.A. Martoglio, Rev. Sci. Instrum. 66 (1995) 1298–1302.
[4] P. Dumas, G.P. Williams, in: T.-K. Sham (Ed.), Chemical Applications of Synchrotron Radiation, Part I: Dynamcis and VUV Spectroscopy, World Scientific Publishing, Singapore, 2002, pp. 356–386.
[5] N.S. Marinkovic, R. Huang, P. Bromberg, M. Sullivan, J. Toomey, L.M. Miller, E. Sperber, S. Moshe, K.W. Jones, E. Chouparova, S. Lappi, S. Franzen, M.R. Chance, J. Synchrotron Radiat. 9 (2002) 189–197.
[6] G.L. Carr, Vib. Spectrosc. 19 (1999) 53–60.
[7] G.L. Carr, Rev. Sci. Instrum. 72 (2001) 1613–1619.
[8] K.S. Kalasinsky, Cell. Mol. Biol. 44 (1998) 81–87.
[9] P. Dumas, J. Phys. IV 104 (2003) 359–364.
[10] I.M. Kempson, W.M. Skinner, P.K. Kirkbride, Biochim. Biophys. Acta 1624 (2003) 1–5.

[11] T.J. Wilkinson, D.L. Perry, M.C. Martin, W.R. McKinney, A.A. Cantu, Appl. Spectrosc. 56 (2002) 800–803.
[12] T.J. Wilkinson, D.L. Perry, M.C. Martin, W.R. McKinney, Proceedings of the 225th American Chemical Society National Meeting, U975–U976 157–IEC Part 1, New Orleans, USA, 2003.
[13] T.J. Wilkinson, D.L. Perry, M.C. Martin, W.R. McKinney, Proceedings of the 225th American Chemical Society National Meeting, U976–U976 158–IEC Part 1, New Orleans, USA, 2003.
[14] E.M. Suzuki, J. Forensic Sci. 44 (1999) 1151–1175.
[15] R.A. Merrill, E.G. Bartick, J. Forensic Sci. 45 (2000) 93–98.
[16] S. Stich, D. Bard, L. Gros, H.W. Wenz, J. Yarwood, K. Williams, J. Raman Spectrosc. 29 (1998) 787–790.
[17] L. Cho, J.A. Reffner, D.L. Wetzel, J. Forensic Sci. 44 (1999) 283–291.
[18] M.W. Tungol, E.G. Bartick, A. Montaser, in: H.J. Humecki (Ed.), Practical Guide to Infrared Microspectroscopy, Marcel Dekker Inc., New York, 1995, pp. 245–286.
[19] L. Cho, J.A. Reffner, B.M. Gatewood, D.L. Wetzel, J. Forensic Sci. 44 (1999) 275–282.
[20] G. Ellis, M.A. Gomez, C. Marco, J. Macromol. Sci. Phys. B43 (2004) 191–206.
[21] Y. Wang, F. DeCarlo, D.C. Mancini, I. McNulty, B. Tieman, J. Bresnahan, I. Foster, J. Insley, P. Lane, G. von Laszewski, C. Kesselman, M.-H. Su, M. Thiebaux, Rev. Sci. Instrum. 72 (2001) 2062–2068.
[22] L. Niewohner, H.W. Wenz, J. Forensic Sci. 44 (1999) 105–109.
[23] D.V. Rao, T. Takeda, T. Kawakami, K. Uesugi, Y. Tsuchiya, J. Wu, T.T. Lwin, Y. Itai, T. Zeniya, T. Yuasa, T. Akatsuka, Nucl. Instrum. Meth. A 523 (2004) 206–216.
[24] M. Kocsis, A. Snigirev, Nucl. Instrum. Meth. A 525 (2004) 79–84.
[25] S.K. Sinha, Radiat. Phys. Chem. 70 (2004) 633–640.
[26] C. Giles, M.G. Honnicke, R.T. Lopes, H.S. Rocha, O.D. Concalves, I. Mazzaro, C. Cusatis, J. Synchrotron Radiat. 10 (2003) 421–423.
[27] J. Baruchel, P. Cloetens, J. Hartwig, W. Ludwig, L. Mancini, P. Pernot, M. Schlenker, J. Synchrotron Radiat. 7 (2000) 196–201.
[28] F. D'Acapito, I. Davoli, P. Ghigna, S. Mobilio, J. Synchrotron Radiat. 10 (2003) 260–264.
[29] F. Xu, W. Liu, S. Wei, C. Xu, G. Pan, X. Zhang, J. Sun, W. Zhao, H. Cui, W. Ye, J. Synchrotron Radiat. 8 (2001) 348–350.
[30] S. Heald, E. Stern, D. Brewe, R. Gordon, D. Crozier, D. Jiang, J. Cross, J. Synchrotron Radiat. 8 (2001) 342–344.
[31] J. Stoehr, NEXAFS Spectroscopy, Springer Verlag, Berlin, 1996.
[32] A.L.D. Kilcoyne, T. Tylisczcak, W.F. Steele, S. Fakra, P. Hitchcock, K. Franck, E. Anderson, B. Harteneck, E.G. Rightor, G.E. Mitchell, A.P. Hitchcock, L. Yang, T. Warwick, H. Ade, J. Synchrotron Radiat. 10 (2003) 125–136.
[33] B. Winn, H. Abe, C. Buckley, M. Feser, M. Howells, S. Hulbert, C. Jacobsen, K. Kaznacheyev, J. Kirz, A. Osanna, J. Maser, I. McNulty, J. Miao, T. Oversluizen, S. Spector, B. Sullivan, Y. Wang, S. Wirick, H. Zhang, J. Synchrotron Radiat. 7 (2000) 395–404.
[34] T. Warwick, H. Ade, D. Kilcoyne, M. Kritscher, T. Tylisczcak, S. Fakra, A. Hitchcock, P. Hitchcock, H. Padmore, J. Synchrotron Radiat. 9 (2002) 254–257.
[35] F. Sirotti, F. Polack, J.L. Cantin, M. Sacchi, R. Delaunay, M. Meyer, M. Liberati, J. Synchrotron Radiat. 7 (2000) 5–11.
[36] C. Jacobsen, S. Wirick, G. Flynn, C. Zimba, J. Microsc. 197 (2000) 173–184.
[37] J. Maser, A. Osanna, Y. Wang, C. Jacobsen, J. Kirz, S. Spector, B. Winn, D. Tennant, J. Microsc. 197 (2000) 68–79.
[38] M. Polentarutti, R. Glazer, K.D. Carugo, J. Appl. Crystallogr. 37 (2004) 319–324.
[39] C.R. Howden, R.J. Dudley, K.W. Smalldon, J. Forensic Sci. Soc. 18 (1978).
[40] S. Ryland, J. Forensic Sci. 31 (1986) 1314–1329.
[41] R.D. Koons, C.A. Peters, P.S. Rebbert, J. Anal. Atom. Spectrom. 6 (1991) 451–456.
[42] J. Kunicki-Goldfinger, J. Kierzek, A. Kasprzak, B. Malozewska-Bucko, X-ray Spectrom. 29 (2000) 310–316.
[43] S. Becker, L. Gunaratnum, T. Hicks, W. Stoecklein, G. Warman, Probl. Forensic Sci. XLVII (2001) 80–92.
[44] T. Hicks, F. Monard Sermier, T. Goldman, A. Brunelle, C. Champod, P. Margot, Forensic Sci. Int. 137 (2003) 107–118.
[45] S. Becker, W. Stoecklein, Trace Session of the Second European Academy of Forensic Sciences Meeting, Cracow, Poland, 2000.
[46] J.R. Almirall, NITECRIME Workshop, Wellington, New Zealand, 2004.
[47] T. Trejos, S. Montero, J.R. Almirall, Anal. Bioanal. Chem. 376 (2003) 1255–1264.
[48] R.J. Watling, Proceedings of the Second European Academy of Forensic Sciences Meeting, Cracow, Poland, 2000.
[49] R.J. Watling, B.F. Lynch, D. Herring, J. Anal. Atom. Spectrom. 12 (1997) 195–203.
[50] R.D. Dixon, R.K.W. Merkle, A. Kijko, NITECRIME Workshop, Wellington, New Zealand, 2004.
[51] R.J. Watling, NITECRIME Workshop, Wellington, New Zealand, 2004.
[52] J.R. Almirall, K.G. Furton, Proceedings of the 16th ANZFSS Symposium on the Forensic Sciences, Canberra, Australia, 2002.
[53] F. Adams, K. Janssens, A. Snigirev, J. Anal. Atom. Spectrom. 13 (1998) 319–331.
[54] K. Janssens, G. Vittiglio, I. Deraedt, A. Aerts, B. Vekemans, L. Vincze, F. Wei, I. Deryck, O. Schalm, F. Adams, A. Rindby, A. Knochel, A. Simionovici, A. Snigirev, X-ray Spectrom. 29 (2000) 73–91.
[55] S. Muratsu, T. Ninomiya, Y. Kagoshima, J. Matsui, J. Forensic Sci. 47 (2002) 944–949.
[56] M.J. Anjos, R.T. Lopes, E.F.O. de Jesus, S. Moreira, R.C. Barroso, C.R.F. Castro, Spectrochim. Acta B 58 (2003) 2227–2232.
[57] A.C.M. Costa, M.J. Anjos, S. Moreira, R.T. Lopes, E.F.O. de Jesus, Spectrochim. Acta B 58 (2003) 2199–2204.
[58] S. Suzuki, Y. Suzuki, M. Kasamatsu, Jpn. Soc. Anal. Chem. 17 (Suppl.) (2001) i163–i164.
[59] I. Nakai, Y. Terada, M. Itou, Y. Sakurai, J. Synchrotron Radiat. 8 (2001) 1078–1081.
[60] Y. Suzuki, M. Kasamatsu, R. Sugita, H. Ohta, S. Suzuki, Y. Marumo, Bunseki Kagaku 52 (2003) 469–474.
[61] Z. Smit, K. Janssens, K. Proost, I. Langus, Nucl. Instrum. Meth. B 219–220 (2004) 35–40.
[62] V. Cherezov, K.M. Riedi, M. Caffrey, J. Synchrotron Radiat. 9 (2002) 333–341.
[63] P. O'Neill, D.L. Stevens, E.F. Garman, J. Synchrotron Radiat. 9 (2002) 329–332.
[64] T. Teng, K. Moffat, J. Synchrotron Radiat. 7 (2000) 313–317.
[65] R. Muller, E. Weckert, J. Zellner, M. Drakopoulos, J. Synchrotron Radiat. 9 (2002) 368–374.
[66] E. Garman, C. Nave, J. Synchrotron Radiat. 9 (2002) 327–328.
[67] R.B.G. Ravelli, P. Theveneau, S. McSweeney, M. Caffrey, J. Synchrotron Radiat. 9 (2002) 355–360.
[68] B.L. Hanson, J.M. Harp, K. Kirschbaum, C.A. Schall, A. DeWitt, A. Howard, A.A. Pinkerton, G.J. Bunick, J. Synchrotron Radiat. 9 (2002) 375–381.
[69] L. Kempenaers, K. Janssens, L. Vincze, B. Vekemans, A. Somogyi, M. Drakopoulos, A. Simionovici, F. Adams, Anal. Chem. 74 (2002) 5017–5026.
[70] P. Philippot, B. Menez, P. Chevallier, F. Gibert, F. Legrand, P. Populus, Chem. Geol. 144 (1998) 121–136.
[71] B. Kanngiesser, Spectrochim. Acta B 58 (2003) 609–614.
[72] J. Kawai, S. Tohno, Y. Kitajima, O.E. Raola, M. Takaoka, Spectrochim. Acta B 58 (2003) 635–639.
[73] B. Charpentier, C. Desrochers, J. Forensic Sci. 45 (2000) 447–452.
[74] J. Brazeau, R.K. Wong, J. Forensic Sci. 42 (1997) 424–428.
[75] J. Flynn, M. Stoilovic, C. Lennard, I. Prior, H. Kobus, Forensic Sci. Int. 97 (1998) 21–36.

[76] L. Vincze, A. Somogyi, J. Osan, B. Vekemans, S. Torok, K. Janssens, F. Adams, Anal. Chem. 74 (2002) 1128.
[77] A. Rindby, K. Janssens, J. Osan, X-ray Spectrom. 32 (2003) 248–257.
[78] A. Ide-Ektessabi, K. Shirasawa, A. Koizumi, M. Azechi, Nucl. Instrum. Meth. B 213 (2004) 761–765.
[79] M.J. Anjos, R.C. Barroso, C.A. Perez, D. Braz, S. Moreira, K.R.H.C. Dias, R.T. Lopes, Nucl. Instrum. Meth. B 213 (2004) 569–573.
[80] I.M. Kempson, W.M. Skinner, P.K. Kirkbride, A.J. Nelson, A.M. Martin, Eur. J. Mass Spectrom. 9 (2003) 589–597.
[81] I.M. Kempson, W.M. Skinner, K.P. Kirkbride, Sci. Total Environ. 9 (2003) 589–597.
[82] T.Y. Toribara, Instrum. Sci. Technol. 23 (1995) 217–226.
[83] I. Nicolis, P. Deschamps, E. Curis, O. Corriol, V. Acar, N. Zerrouk, J.C. Chaumeil, F. Guyon, S. Benazeth, J. Synchrotron Radiat. 8 (2001) 984–986.
[84] L. Bertrand, J. Doucet, P. Dumas, A. Simionovici, G. Tsoucaris, P. Walter, J. Synchrotron Radiat. 10 (2003) 387–392.
[85] K. Geraki, M.J. Farquharson, D.A. Bradley, R.P. Hugtenburg, Nucl. Instrum. Meth. B 213 (2004) 564–568.
[86] N.Q. Liu, F. Zhang, X.F. Wang, Z.Y. Zhang, Z.F. Chai, Y.Y. Huang, W. He, X.Q. Zhao, A.J. Zuo, R. Yang, Spectrochim. Acta B 59 (2004) 255–260.
[87] A.J. Berry, H.S.C. O'Neill, K.D. Jayasuriya, S.J. Campbell, G.J. Foran, Am. Mineral. 88 (2003) 967–977.
[88] L. Galoisy, G. Calas, M.A. Arrio, Chem. Geol. 174 (2001) 307–319.
[89] M. Bonnin-Mosbah, A.S. Simionovici, N. Metrich, J.P. Duraud, D. Massare, P. Dillmann, J. Non-Cryst. Solids 288 (2001) 103–113.
[90] G. Hellmiss, W. Lichtenberg, M. Weiss, J. Forensic Sci. 32 (1987) 747–760.
[91] A. Zeichner, B. Schecter, R. Brener, J. Forensic Sci. 43 (1998) 493–501.
[92] J. Coumbaros, K.P. Kirkbride, G. Klass, W. Skinner, Forensic Sci. Int. 119 (2001) 72–81.
[93] P. Collins, J. Coumbaros, G. Horsley, B. Lynch, P.K. Kirkbride, W. Skinner, G. Klass, J. Forensic Sci. 48 (2003).
[94] T.E. Westre, P. Kennepohl, J.G. DeWitt, B. Hedman, K.O. Hodgson, E.I. Solomon, J. Am. Chem. Soc. 119 (1997) 6297–6314.
[95] J. Kawai, K. Hayakawa, S.Y. Zheng, Y. Kitajima, H. Adachi, Y. Gohshi, F. Esaka, K. Furuya, Physica B 209 (1995) 237–238.
[96] J. Kawai, S. Hayakawa, F. Esaka, S.Y. Zheng, Y. Kitajima, K. Maeda, H. Adachi, Y. Gohshi, K. Furuya, Anal. Chem. 67 (1995) 1526–1529.
[97] Z.Y. Wu, M. Bonnin-Mosbah, J.P. Duraud, N. Metrich, J.S. Delaney, J. Synchrotron Radiat. 6 (1999) 344–346.
[98] X. Li, J.A. Monroe Snider, D. Schiferl, PPG Technol. J. 5 (1999) 31–41.
[99] K. Proost, K. Janssens, B. Wagner, E. Bulska, M. Schreiner, Nucl. Instrum. Meth. B 213 (2004) 723–728.
[100] J. Coumbaros, Thesis, Ian Wark Research Institute, University of South Australia, Adelaide, 2002.
[101] F.E. Huggins, G.P. Huffman, J.D. Robertson, J. Hazard. Mater. 74 (2000) 1–23.
[102] Y. Shimizugawa, J.R. Qui, K. Hirao, J. Non-Cryst. Solids 222 (1997) 310–315.
[103] E. Welter, W. Calmano, S. Mangold, L. Troger, Fresenius J. Anal. Chem. 364 (1999) 238–244.
[104] M.L. Peterson, G.E. Brown, G.A. Parks, J. Phys. IV 7 (1997) 781–783.
[105] M.I. Boyanov, S.D. Kelly, K.M. Kemner, B.A. Bunker, J.B. Fein, D.A. Fowle, Geochim. Cosmochim. Acta 67 (2003) 3299–3311.
[106] D.G. Strawn, D.L. Sparks, Soil Sci. Soc. Am. J. 64 (2000) 144–156.
[107] A. Manceau, M.A. Marcus, N. Tamura, O. Proux, N. Geoffroy, B. Lanson, Geochim. Cosmochim. Acta 68 (2004) 2467–2483.
[108] C.M.B. Henderson, G. Cressey, S.A.T. Redfern, Radiat. Phys. Chem. 45 (1995) 459–481.
[109] M. Tassa, Y. Leist, M. Steinberg, J. Forensic Sci. 27 (1982) 677–683.
[110] A. Ruffell, P. Wiltshire, Forensic Sci. Int. 145 (2004) 13–23.
[111] D.F. Rendle, Rigaku J. 19–20 (2003) 11–22.
[112] T. Broekmans, A. Adriaens, E. Pantos, Nucl. Instrum. Meth. B 226 (2004) 92–97.
[113] E. Dooryhee, P. Martinetto, P. Walter, M. Anne, Radiat. Phys. Chem. 71 (2004) 863–868.
[114] M.A. Marcus, A.A. MacDowell, R. Celestre, A. Manceau, T. Miller, H.A. Padmore, R.E. Sublett, J. Synchrotron Radiat. 11 (2004) 239–247.
[115] M. Knapp, C. Baehtz, H. Ehrenberg, H. Fuess, J. Synchrotron Radiat. 11 (2004) 328–334.
[116] C. Meneghini, G. Artioli, A. Balerna, A.F. Gualtieri, P. Norby, S. Mobilio, J. Synchrotron Radiat. 8 (2001) 1162–1166.
[117] T. Ikeda, A. Nisawa, M. Okui, N. Yagi, H. Yoshikawa, S. Fukushima, J. Synchrotron Radiat. 10 (2003) 424–429.
[118] A. Martorana, G. Deganello, A. Longo, F. Deganello, L. Liotta, A. Macaluso, G. Pantaleo, A. Balerna, C. Meneghini, S. Mobilio, J. Synchrotron Radiat. 10 (2003) 177–182.
[119] C. Riekel, J. Synchrotron Radiat. 11 (2004) 4–6.
[120] W.R. Wikoff, W. Schildkamp, R.E. Johnson, Acta Crystallogr. D 56 (2000) 890–893.
[121] H. Renevier, S. Grenier, S. Arnaud, J.F. Berar, B. Caillot, J.L. Hodeau, A. Letoublon, M.G. Proietti, B. Ravel, J. Synchrotron Radiat. 10 (2003) 435–444.
[122] E. Pohl, A. Gonzalez, C. Hermes, R.G. van Silfhout, J. Synchrotron Radiat. 8 (2001) 1113–1120.
[123] M. Roth, P. Carpentier, O. Kaikati, J. Joly, P. Charrault, M. Pirocchi, R. Kahn, E. Fanchon, L. Jacquamet, F. Borel, A. Bertoni, P. Israel-Gouy, J.-L. Ferrer, Acta Crystallogr. D58 (2002) 805–814.
[124] J. Ohana, L. Jacquamet, J. Joly, A. Bertoni, P. Taunier, L. Michel, P. Charrault, M. Pirocchi, P. Carpentier, F. Borel, R. Kahn, J.-L. Ferrer, J. Appl. Crystallogr. 37 (2004) 72–77.
[125] L. Jacquamet, J. Ohana, J. Joly, P. Legrand, R. Kahn, F. Borel, M. Pirocchi, P. Charrault, P. Carpentier, J.-L. Ferrer, Acta Crystallogr. D60 (2004) 888–894.
[126] A. Olczak, M. Cianci, Q. Hao, P.J. Rizkallah, J. Raftery, J.R. Helliwell, Acta Crystallogr. A59 (2003) 327–334.
[127] R.J. Cernik, P. Barnes, G. Bushnell-Wye, A.J. Dent, G.P. Diakun, J.V. Flaherty, G.N. Greaves, E.L. Heeley, W. Helsby, S.D.M. Jacques, J. Kay, T. Rayment, A. Ryan, C.C. Tang, N.J. Terrill, J. Synchrotron Radiat. 11 (2004) 163–170.
[128] T.R. Welberry, D.J. Goossens, D.R. Haeffner, P.L. Lee, J. Almer, J. Synchrotron Radiat. 10 (2003) 284–286.
[129] G. Tirao, G. Stutz, C. Cusatis, J. Synchrotron Radiat. 11 (2004) 335–342.
[130] J.C. Hiller, T.J.U. Thompson, M.P. Evison, A.T. Chamberlain, T.J. Wess, Biomaterials 24 (2003) 5091–5097.
[131] L. Kempenaers, L. Vincze, K. Janssens, Spectrochim. Acta B 55 (2000) 651–669.
[132] L. Kempenaers, K. Janssens, K.P. Jochum, L. Vincze, B. Vekemans, A. Somogyi, M. Drakopoulos, F. Adams, J. Anal. Atom. Spectrom. 18 (2003) 350–357.
[133] S.M. Eggins, J.M.G. Shelley, Geostandard. Newslett. 26 (2002) 269–286.
[134] J. Prietzel, J. Thieme, U. Neuhausler, J. Susini, I. Kogel-Knabner, Eur. J. Soil Sci. 54 (2003) 423–433.
[135] C. Torre, G. Mattutino, V. Vasino, C. Robino, J. Forensic Sci. 47 (2002) 494–594.
[136] F.S. Romolo, P. Margot, Forensic Sci. Int. 119 (2001).
[137] S. Heald, D. Jiang, in: T.K. Sham (Ed.), Chemical Applications of Synchrotron Radiation. Part II: X-ray Applications, World Scientific Publishing Co. Pty. Ltd., Singapore, 2002, pp. 761–798.